

Complete bolometric treatment of irradiation effects:  
general discussion and application to binary stars

MARTIN HORVAT,<sup>1,2</sup> KYLE E. CONROY,<sup>2</sup> DAVID JONES,<sup>3,4</sup> AND ANDREJ PRŠA<sup>2</sup>

<sup>1</sup>*University of Ljubljana, Dept. of Physics, Jadranska 19, SI-1000 Ljubljana, Slovenia*

<sup>2</sup>*Villanova University, Dept. of Astrophysics and Planetary Sciences, 800 E Lancaster Ave, Villanova PA 19085, USA*

<sup>3</sup>*Instituto de Astrofísica de Canarias, E-38205 La Laguna, Tenerife, Spain*

<sup>4</sup>*Departamento de Astrofísica, Universidad de La Laguna, E-38206 La Laguna, Tenerife, Spain*

ABSTRACT

A general framework for dealing with irradiation effects in the bolometric sense is presented. Specifically, reflection with heat absorption and consequent redistribution of the absorbed heat, for systems of astrophysical bodies where the boundaries are used as support for the description of the processes. Discussed are its mathematical and physical properties, as well as its implementation approximations, with a focus on three plausible redistribution processes (uniform, latitudinal and local redistribution). These are tested by extending PHOEBE 2.1 (<http://phoebe-project.org/>), the open source package for modeling eclipsing binaries, and applied to a toy model of the known two-body eclipsing systems.

*Keywords:* Methods: analytical, numerical; Techniques: photometric, Binaries: eclipsing; Stars: fundamental parameters

1. INTRODUCTION

There are at least three fundamentally different approaches for dealing with the reflection effect in binary stars. The most precise, and typically most time-consuming, approach is to treat the stellar atmospheres in detail and use radiative transfer to calculate new temperatures and fluxes emitted from each of the stars (see e.g. Nordlund & Vaz 1990; Hubeny et al. 2003). A much simpler, but less precise, treatment can be achieved by using standard (non-irradiated) model atmospheres to approximate the flux emitted from the individual stars, which is then reflected between surfaces multiple times and thereby effectively heating the surfaces. The most widely spread example of such an approach is the Wilson reflection model (Wilson 1990). For a very illustrative description of the latter see, e.g., Kallrath & Milone (2009). However, un-

der this scheme energy is not always conserved, with some fraction of the incident flux being reflected while the rest is essentially ignored. To the best of our knowledge, the first model that addresses this issue, combining reflection with redistribution of absorbed energy across the surfaces, is presented by [Budaj \(2011\)](#) and implemented in the SHELLSPEC code [Budaj & Richards \(2004\)](#). Their model focuses on an effective description of uniform and latitudinal redistribution in Roche geometry. Finally, the fastest and arguably least informative methodology for approximating irradiation is based on relative corrections of the observables due to reflection. Such an approach was used in [Barclay et al. \(2012\)](#) and [Barclay et al. \(2015\)](#), where they take an analytic model for light curves in binary systems of spherical bodies with quadratic limb darkening, provided by the [Mandel & Agol \(2002\)](#) transit model, and account for reflection by correcting the observed flux by a simple and analytic phase dependent multiplicative factor.

We present a consistent mathematical model for handling the reflection effect from astrophysical bodies with redistribution of the absorbed irradiation in the directions laid out by [Budaj \(2011\)](#). We refer to these combined effects as irradiation effects. We consider only stationary or quasi-stationary redistribution, where we assume that the energy balance is fulfilled at all times, but the redistribution rules may change in time. If these changes are slow in comparison to the flux transport, the quasi-stationary assumption is physically justified. In addition, we assume that the redistribution does not significantly change the limb-darkening law of the considered surface (a necessary assumption given that redefining the limb-darkening would require detailed treatment of irradiation in the stellar atmosphere models; [Claret 2007](#)). Our discussion is limited to the purely bolometric treatments of irradiation effects with (Bond)<sup>1</sup> bolometric albedo depending on the position on the surface. Nevertheless, we acknowledge that such a bolometric albedo is a poor representation of the effective albedo, which is essentially wavelength and temperature dependent ([Vaz & Nordlund 1985](#)). The bolometric albedo is generally assumed to be non-unity, which is discussed in [Ruciński \(1969\)](#) for different types of stellar envelopes. As highlighted above, the energy balance in several standard reflection models e.g [Wilson \(1990\)](#), [Prša & Zwitter \(2005\)](#) is violated when deviating from unity bolometric albedo.

The reflection-redistribution (or simply irradiation) framework presented here is tested by extending the publicly accessible Python package PHOEBE available at <http://phoebe-project.org/>, which internally handles limb darkening, Doppler shifts, and other details that determine emission properties of the considered astrophysical bodies. As the bolometric process discussed here is quite limiting for applications, this paper is not accompanied with a new release of the code. If a passband treatment is developed in the future, the code will be released at that time. This work can be considered a generalization of reflection-redistribution model introduced by [Budaj](#)

<sup>1</sup> Here the albedo is assumed to lie in the range  $[0,1]$  and is sometimes called Bond albedo to differentiate from the geometric albedo.

(2011), making it more geometry independent and easily extendable with different redistribution types.

We start the paper by introducing some common notation to describe the irradiation processes which are then used to define different reflection schemes and redistribution effects. Our description relies heavily on linear operators that make expressions more compact and readable, and compatible with modern implementations. We then explain the discretization of the introduced operators on triangular surfaces and outline practical considerations relating to the implementation of irradiation schemes. We conclude the paper with demonstrations of these principles on a toy model binary system.

## 2. DESCRIPTION OF IRRADIATION

Each body forms a closed boundary,  $\mathcal{M}_i$ . The union of all such boundaries constitutes the *topological surface*  $\mathcal{M} = \bigcup_i \mathcal{M}_i$ . Let us define a visibility function  $V(\mathbf{r}, \mathbf{r}')$  between the two points  $\mathbf{r}, \mathbf{r}' \in \mathcal{M}$  as:

$$V(\mathbf{r}, \mathbf{r}') = \begin{cases} 1 & : \text{line of sight } \mathbf{r} \leftrightarrow \mathbf{r}' \text{ is unobstructed} \\ 0 & : \text{otherwise} \end{cases} .$$

In a system of two convex bodies, this visibility function is given by

$$V(\mathbf{r}, \mathbf{r}') = U(\hat{\mathbf{e}}(\mathbf{r}, \mathbf{r}') \cdot \hat{\mathbf{n}}(\mathbf{r})) U(\hat{\mathbf{e}}(\mathbf{r}', \mathbf{r}) \cdot \hat{\mathbf{n}}(\mathbf{r}')) , \quad (1)$$

where  $U(x) = \{1 : x \geq 0; 0 : \text{otherwise}\}$  is the step-function.

In order to facilitate the discussion that follows, we start with a concise glossary of the frequently used radiometric terms. Further details are provided by [Modest \(2013\)](#).

**Intensity:** energy flux in the direction  $\hat{\mathbf{e}}$  from point  $\mathbf{r}$  on the surface per solid angle per unit area normal to the surface and is here denoted by  $I(\hat{\mathbf{e}}, \mathbf{r})$ . In modern radiometry literature this quantity is usually called the radiance and the intensity is then defined as the surface integral of the radiance. It is also referred to as bolometric intensity or total intensity in [Modest \(2013\)](#).

**Irradiance:** radiant flux per unit area intercepted by a surface at a certain point  $\mathbf{r}$ , denoted by  $F_{\text{irr}}(\mathbf{r})$  or  $F_{\text{in}}(\mathbf{r})$ , with the index indicating that the energy flux is directed towards the surface.

**Radiant exitance:** energy flux emitted at a certain point  $\mathbf{r}$  on a surface per unit area. The quantity is denoted by  $F_{\text{ext}}(\mathbf{r})$  in general, or  $F_0(\mathbf{r})$  if we talk about intrinsic exitance, or  $F'_0(\mathbf{r})$  if we talk about intrinsic exitance after taking into account the redistribution of irradiation. Radiant exitance is frequently referred to only as exitance.

**Radiosity:** total energy flux per unit area that leaves (is emitted, reflected and transmitted) a certain point  $\mathbf{r}$  on the surface. It is denoted by  $F_{\text{out}}(\mathbf{r})$ , with the index indicating that the energy flux is directed away from the surface.

**Reflection:** a process by which a part of the energy flux received by the surface is transmitted or emitted back into space, depending on the reflection model.

**Redistribution:** a process by which the absorbed energy flux at the surface, i.e. the part of the flux which is not reflected, is redistributed across the surface. This additional energy flux is subsequently re-emitted from the surface.

The intensity  $I(\hat{\mathbf{e}}, \mathbf{r})$  (i.e. flux per unit solid angle per projected unit area) defined for each point  $\mathbf{r}$  on the surface  $\mathcal{M}$  is:

$$I(\hat{\mathbf{e}}, \mathbf{r}) = \frac{\partial \Phi}{\partial \Omega \partial A \cos \theta}, \quad \cos \theta = \hat{\mathbf{e}} \cdot \hat{\mathbf{n}}(\mathbf{r}),$$

where  $\hat{\mathbf{e}}$  ( $\|\hat{\mathbf{e}}\| = 1$ ) is the direction of emission and  $\hat{\mathbf{n}}(\mathbf{r})$  represents the normal vector on the surface pointing outward at point  $\mathbf{r}$ . The *irradiance*  $F_{\text{irr}}$  depends on the intensity (i.e. the radiant flux incident on the surface, per unit area, is due to the intensity; cf. Prša et al. 2016) at each point  $\mathbf{r} \in \mathcal{M}$  as:

$$F_{\text{irr}}(\mathbf{r}) = \int_{\mathcal{M}} V(\mathbf{r}, \mathbf{r}') \frac{(\hat{\mathbf{e}}(\mathbf{r}', \mathbf{r}) \cdot \hat{\mathbf{n}}(\mathbf{r}))(\hat{\mathbf{e}}(\mathbf{r}, \mathbf{r}') \cdot \hat{\mathbf{n}}(\mathbf{r}'))}{|\mathbf{r} - \mathbf{r}'|^2} I(\hat{\mathbf{e}}(\mathbf{r}, \mathbf{r}'), \mathbf{r}') dA(\mathbf{r}') \quad (2)$$

$$\equiv \hat{\mathcal{Q}}I(\mathbf{r}), \quad (3)$$

with  $\hat{\mathbf{e}}(\mathbf{r}, \mathbf{r}') = \widehat{\mathbf{r} - \mathbf{r}'}$  denoting a unit-vector pointing from  $\mathbf{r}'$  to  $\mathbf{r}$ . For simplicity we introduce the irradiation operator  $\hat{\mathcal{Q}}$  for mapping intensities to irradiances.

If we assume that the surface behaves as a Lambertian radiator, then the intensity  $I$  is described by the Lambert cosine law (Hapke 2012, Ch. 8.5.1):

$$I(\hat{\mathbf{e}}, \mathbf{r}) = I_0(\mathbf{r}).$$

The resulting *radiant exitance* (i.e. the radiant flux emitted from a unit area of the surface) is given by:

$$F_{\text{ext}}(\mathbf{r}) = \int_{\hat{\mathbf{n}} \cdot \hat{\mathbf{e}} \geq 0} I(\hat{\mathbf{e}}, \mathbf{r}) (\hat{\mathbf{e}} \cdot \hat{\mathbf{n}}) d\Omega(\hat{\mathbf{e}}) = \pi I_0(\mathbf{r}).$$

By using the connection between intensity and exitance, we can express the irradiance  $F_{\text{irr}}$  as a function of the exitance  $F_{\text{ext}}$  by introducing a Lambertian *radiosity* operator  $\hat{\mathcal{L}}_{\text{L}}$ :

$$F_{\text{irr}} = \hat{\mathcal{L}}_{\text{L}} F_{\text{ext}} \quad \hat{\mathcal{L}}_{\text{L}} = \frac{1}{\pi} \hat{\mathcal{Q}}. \quad (4)$$

Radiosity operators are commonly used in computer graphics (cf. Gershbein et al. 1994; Cohen & Wallace 2016).

The limb-darkened intensity can be written as:

$$I(\hat{\mathbf{e}}, \mathbf{r}) = I_0(\mathbf{r})D(\hat{\mathbf{e}} \cdot \hat{\mathbf{n}}, \mathbf{r}), \quad (5)$$

where  $I_0(\mathbf{r})$  is the normal emergent intensity and  $D$  is the limb-darkening factor;  $D(1, \mathbf{r}) = 1$ . The corresponding radiant exitance then becomes:

$$F_{\text{ext}}(\mathbf{r}) = \int_{\hat{\mathbf{n}} \cdot \hat{\mathbf{e}} \geq 0} I(\hat{\mathbf{e}}, \mathbf{r}) (\hat{\mathbf{e}} \cdot \hat{\mathbf{n}}) d\Omega(\hat{\mathbf{e}}) = I_0(\mathbf{r})D_0(\mathbf{r}), \quad (6)$$

with integrated limb-darkening factor over the hemisphere

$$D_0(\mathbf{r}) = \int_{\hat{\mathbf{n}} \cdot \hat{\mathbf{e}} \geq 0} D(\hat{\mathbf{e}} \cdot \hat{\mathbf{n}}, \mathbf{r}) (\hat{\mathbf{e}} \cdot \hat{\mathbf{n}}) d\Omega(\hat{\mathbf{e}}). \quad (7)$$

We can now close the loop by expressing irradiation with radiant exitance by introducing the limb-darkened radiosity operator  $\hat{\mathcal{L}}_{\text{LD}}$ :

$$F_{\text{irr}} = \hat{\mathcal{L}}_{\text{LD}} F_{\text{ext}} \quad \hat{\mathcal{L}}_{\text{LD}} = \hat{\mathcal{Q}} \circ \frac{D}{D_0}. \quad (8)$$

The radiosity operators  $\hat{\mathcal{L}}_{\text{L}}$  and  $\hat{\mathcal{L}}_{\text{LD}}$  are an elegant mathematical way of expressing the relation between the two non-directional quantities, i.e., irradiation and exitance.

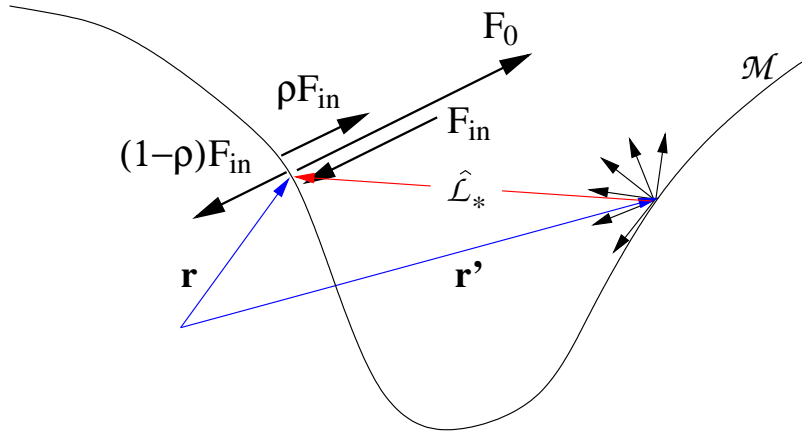


**Figure 1.** Illustration of the irradiation  $F_{\text{in}}$  calculated through the radiosity operators  $\hat{\mathcal{L}}_*$ , with  $*$  = L or LD; where at point  $\mathbf{r}$  the reflected part of the irradiation is  $\rho(\mathbf{r})F_{\text{in}}(\mathbf{r})$  and the absorbed part is  $(1 - \rho(\mathbf{r}))F_{\text{in}}(\mathbf{r})$ .

### 3. REFLECTION MODELS

Let us assume that we know the intrinsic exitance  $F_0$  and the reflection fraction  $\rho$  (i.e. the ratio of the incoming energy flux per unit area that is reflected) for each point on the surface  $\mathcal{M}$ . The intrinsic exitance irradiates the unobstructed surface, some of which reflects back and irradiates the radiating surface, iteratively. We quantify the resulting radiosity (i.e. the radiant flux leaving the surface per unit area)  $F_{\text{out}}$  by introducing a reflection model.

We discuss two reflection models in detail: that proposed by [Wilson \(1990\)](#), and the Lambertian model introduced by [Prša et al. \(2016\)](#). [Wilson's](#) model is based on the following set of equations:

$$F_{\text{in}} = \hat{\mathcal{L}}_{\text{LD}} F_{\text{out}} \quad F_{\text{out}} = F_0 + \hat{\Pi} F_{\text{in}}, \quad (9)$$

while [Prša et al.](#)'s reflection model is based on the following set:

$$F_{\text{in}} = \hat{\mathcal{L}}_{\text{LD}} F_0 + \hat{\mathcal{L}}_{\text{L}} \hat{\Pi} F_{\text{in}} \quad F_{\text{out}} = F_0 + \hat{\Pi} F_{\text{in}}, \quad (10)$$

where  $\hat{\mathcal{L}}_{\text{LD}}$  and  $\hat{\mathcal{L}}_{\text{L}}$  are the radiosity operators introduced by Eqs. (8) and (4), respectively. Additionally, we introduce reflection operator  $\hat{\Pi} : f \mapsto \rho f$ , with  $\rho$  being a scalar function defined on the surface describing the local (Bond) bolometric albedo, i.e., the ratio of reflected light for each point separately.

The set of Eqs. (10) can be combined into a single expression for radiosity  $F_{\text{out}}$ :

$$F_{\text{out}} = [\mathbb{1} + \hat{\Pi}(\hat{\mathcal{L}}_{\text{LD}} - \hat{\mathcal{L}}_{\text{L}})] F_0 + \hat{\Pi} \hat{\mathcal{L}}_{\text{L}} F_{\text{out}}. \quad (11)$$

It is evident from this expression that [Prša et al.](#)'s model reduces to [Wilson's](#) in the limit  $\hat{\mathcal{L}}_{\text{LD}} = \hat{\mathcal{L}}_{\text{L}}$ . In [Wilson's](#) model the radiation from the surface is distributed as a limb-darkened intensity, while in [Prša et al.](#)'s approach only the intrinsic part of the radiance is distributed according to the limb-darkened intensity, while the reflected irradiance is distributed according to the Lambertian cosine law. [Appendix A](#) provides these equations in integral form for the case of two convex radiators.

These reflection models do not conserve energy because the absorbed part of the irradiance,  $(1 - \rho)F_{\text{in}}$ , is dropped from the energy balance. When fitting models to the data, this energy loss can be compensated by increasing the albedo or the effective temperature of the radiators.

#### 4. STATIONARY AND QUASI-STATIONARY REDISTRIBUTION

The redistribution of the incoming energy flux depends on the thermodynamical circumstances in stellar photospheres, i.e. mechanical flows of matter and lateral thermal gradients, which can be very complex. However, for as long as these circumstances are long-lived insofar that we can assume stationary or quasi-stationary equilibrium for each star, we can build a framework to describe the redistribution of energy. We present such a framework and provide approximations for several simple scenarios. We define redistribution as a linear mapping of the incident flux density onto the radiated flux density, both defined on the surface of the body. The linearity assumption implies that the redistribution processes are independent from the flux scaling factors.

##### 4.1. Lossless reflection-redistribution models

We are primarily focusing on radiating bodies with a simple geometry, especially close-to-spherical, where we can describe the redistribution processes and identify

the surface parts associated with flux incidence and emission. For strongly deformed bodies, such as contact binaries, we currently lack sufficient insight to propose a realistic yet tractable model because, as of yet, the thermodynamical properties are not well understood. Substantial effort to better understand radiative transfer in strongly deformed bodies is underway (Kochoska et al. 2018, submitted).

In the stationary or quasi-stationary state we assume that the flux is strictly conserved at all times, meaning that the net incident flux is also emitted at the same time. The absorbed part of the irradiance,  $(1 - \rho)F_{\text{in}}$ , is redistributed over the entire surface and it increases the intrinsic exitance by  $\delta F_0$ . We can describe flux redistribution by defining a redistribution operator  $\hat{\mathcal{D}}$ :

$$\delta F_0 = \hat{\mathcal{D}}[(1 - \rho)F_{\text{in}}] = \hat{\mathcal{D}}(\mathbb{1} - \hat{\Pi})F_{\text{in}}. \quad (12)$$

This redistribution operator could in principle be time-dependent in the quasi-stationary case, but for the strictly stationary state redistribution, the operator does not depend on time. The increased intrinsic exitance  $F'_0$  can be written as:

$$F'_0 = F_0 + \delta F_0 \quad F_{\text{out}} = F'_0 + \hat{\Pi}F_{\text{in}}. \quad (13)$$

By construction, the redistribution operator  $\hat{\mathcal{D}}$  maps positive-valued functions defined over the surface to positive-valued functions and conserves their integrals over the surface.

Generally, we can write the redistribution operator  $\hat{\mathcal{D}}$  at time  $t$  as:

$$\hat{\mathcal{D}}f(\mathbf{r}) = \int_{\mathcal{M}} K(\mathbf{r}, \mathbf{r}'; t) f(\mathbf{r}') dA(\mathbf{r}'),$$

where  $K : \mathcal{M} \times \mathcal{M} \rightarrow \mathbb{R}_+$  is a positive kernel with the following normalization property:

$$\int_{\mathcal{M}} K(\mathbf{r}, \mathbf{r}'; t) dA(\mathbf{r}) = 1 \quad \forall \mathbf{r} \in \mathcal{M}.$$

This imposes the conservation of total flux at a given moment in time over the surface:

$$\int_{\mathcal{M}} [\hat{\mathcal{D}}f](\mathbf{r}) dA(\mathbf{r}) = \int_{\mathcal{M}} f(\mathbf{r}) dA(\mathbf{r}). \quad (14)$$

More generally, we can formulate the kernel by using an auxiliary function  $G : \mathcal{M} \times \mathcal{M} \rightarrow \mathbb{R}_+$ :

$$K(\mathbf{r}, \mathbf{r}'; t) = \frac{G(\mathbf{r}, \mathbf{r}'; t)}{\int_{\mathcal{M}} G(\mathbf{r}, \mathbf{r}'; t) dA(\mathbf{r})}.$$

When the flux is uniformly distributed over the whole surface,  $G_{\text{uniform}} \equiv 1$  and the redistribution operator  $\hat{\mathcal{D}}$  is very simple:

$$\hat{\mathcal{D}}f(\mathbf{r}) = \frac{1}{A} \int_{\mathcal{M}} f(\mathbf{r}') dA(\mathbf{r}').$$

We model a local redistribution by introducing a distance measure (e.g. a geodesic) on the surface,  $d : \mathcal{M} \times \mathcal{M} \rightarrow \mathbb{R}_+$ , and a weight function,  $g : \mathbb{R}_+ \rightarrow \mathbb{R}_+$ , that determines the ratio of the flux that is transported from the irradiated element to any other element on the surface at distance  $d$ . Then the kernel describing the redistribution of incident flux is written as:

$$G_{\text{local}}(\mathbf{r}, \mathbf{r}'; t) = g(d(\mathbf{r}, \mathbf{r}')) . \quad (15)$$

The weight function  $g$  depends on the energy transport in the atmosphere, which we do not (readily) know. However, we can make reasonable assumptions that are likely to hold. Namely, we take  $g$  to be monotonically decreasing and diminishing to zero for arguments larger than a given threshold value  $l$ , for example  $g(x) = \exp(-x/l)$  or  $g(x) = 1 - x/l$ , where  $l$  is proportional to the optical depth in the atmosphere. In the limit  $l \rightarrow 0$ , local redistribution reflects all incoming flux:  $\hat{\mathcal{D}}_{\text{local}, l=0} = \mathbb{1}$ . Therefore, local redistribution with small  $l$  (w.r.t. to the size of object) will have an effect similar to increasing reflection.

In the case of rotating stars, the axis of rotation breaks the isotropic symmetry, so excess flux tends to be reradiated at latitudes similar to where it was received. This gives rise to flux conservation in the latitudinal direction. It is meaningful to define a distance on the surface,  $d_{\perp} : \mathcal{M} \times \mathcal{M} \rightarrow \mathbb{R}_+$ , along the rotation axis  $\hat{\mathbf{s}}$ . The kernel can then be written as:

$$G_{\text{latitudinal}}(\mathbf{r}, \mathbf{r}'; t) = g(d_{\perp}(\mathbf{r}, \mathbf{r}'; \hat{\mathbf{s}})) . \quad (16)$$

Let us make a small digression here and note that, in the case of a phase delay between heating and reradiation, it is possible to incorporate the lag into the presented framework by using coordinates shifted horizontally w.r.t. the rotation axis  $\hat{\mathbf{s}}$ . The kernel for that case would be written as:

$$G_{\text{shift}}(\mathbf{r}, \mathbf{r}'; t) = G(\mathbf{R}_{\phi\hat{\mathbf{s}}}\mathbf{r}, \mathbf{r}'; t) ,$$

where  $\phi$  is the angle by which the location of irradiated element is shifted relative to the location of the radiating element, and  $\mathbf{R}_{\omega}$  is the rotation matrix about the axis of rotation  $\omega$ . We expect that the angle  $\phi$  is positive and proportional to the angular velocity of the star; in general it can also depend on the position and time, as long as the quasi-stationarity of redistribution assumed here is not violated. Note that the horizontal shift does not affect the overall energy balance.

We can describe individual redistribution processes by the corresponding operator  $\hat{\mathcal{D}}_i$  and form the overall redistribution operator  $\hat{\mathcal{D}}$  as a weighted sum of individual  $\hat{\mathcal{D}}_i$ :

$$\hat{\mathcal{D}} = \sum_i w_i \hat{\mathcal{D}}_i, \quad \sum_i w_i = 1 , \quad (17)$$

where  $w_i$  are positive real numbers. We can view Eq. (17) as the decomposition of the redistribution operator  $\hat{\mathcal{D}}$  into generators of a certain type of redistribution, where the weights quantify the amount of energy redistributed by the corresponding process.



Radiosity for [Wilson's](#) model can be obtained by substituting  $F'_0$  from Eq. (13) into Eqs. (9):

$$F_{\text{out}} = F_0 + [\hat{\mathcal{D}}(\mathbb{1} - \hat{\Pi}) + \hat{\Pi}] \hat{\mathcal{L}}_{\text{LD}} F_{\text{out}}. \quad (18)$$

In turn, the updated intrinsic exitance  $F'_0$  is given by the radiosity:

$$F'_0 = F_0 + \hat{\mathcal{D}}(\mathbb{1} - \hat{\Pi}) \hat{\mathcal{L}}_{\text{LD}} F_{\text{out}}. \quad (19)$$

Similarly, irradiation for the Lambertian reflection model can be written as:

$$F_{\text{in}} = \hat{\mathcal{L}}_{\text{LD}} F_0 + [\hat{\mathcal{L}}_{\text{LD}} \hat{\mathcal{D}}(\mathbb{1} - \hat{\Pi}) + \hat{\mathcal{L}}_{\text{L}} \hat{\Pi}] F_{\text{in}}. \quad (20)$$

The solution of these equations determines the intrinsic exitance  $F'_0$  and radiosity  $F_{\text{out}}$ :

$$F'_0 = F_0 + \hat{\mathcal{D}}(\mathbb{1} - \hat{\Pi}) F_{\text{in}}, \quad F_{\text{out}} = F'_0 + \hat{\Pi} F_{\text{in}}. \quad (21)$$

The solutions of the irradiation models, i.e., the updated exitance  $F'_0$  and radiosity  $F_{\text{out}}$ , determine *bolometric* intensity of the radiating bodies. For [Wilson's](#) model, the limb-darkened intensity from Eq. (5) yields:

$$I(\hat{\mathbf{e}}, \mathbf{r}) = \frac{F_{\text{out}}(\mathbf{r})}{D_0(\mathbf{r})} D(\hat{\mathbf{e}}, \mathbf{r}) \quad (22)$$

while for the Lambertian reflection model we get:

$$I(\hat{\mathbf{e}}, \mathbf{r}) = \frac{F'_0(\mathbf{r})}{D_0(\mathbf{r})} D(\hat{\mathbf{e}}, \mathbf{r}) + \frac{F_{\text{out}}(\mathbf{r}) - F'_0(\mathbf{r})}{\pi}. \quad (23)$$

The presented Lambertian irradiation (reflection and redistribution) model is an *exact* bolometric description of this process under two assumptions: (1) Lambertian reflection is wavelength-independent, and (2) redistribution does not affect the limb-darkening of the surface.

To quantify the impact of Lambertian correction, we can expand the updated intrinsic emission  $F'_0$  and radiosity  $F_{\text{out}}$ . For [Wilson's](#) model we get:

$$\begin{aligned} F_{\text{out}} = & F_0 + [\hat{\Pi} + \hat{\mathcal{D}}(\mathbb{1} - \hat{\Pi})] \hat{\mathcal{L}}_{\text{LD}} F_0 + \\ & + [\hat{\Pi} + \hat{\mathcal{D}}(\mathbb{1} - \hat{\Pi})] \hat{\mathcal{L}}_{\text{LD}} [\hat{\Pi} + \hat{\mathcal{D}}(\mathbb{1} - \hat{\Pi})] \hat{\mathcal{L}}_{\text{LD}} F_0 + \dots, \end{aligned} \quad (24)$$

$$\begin{aligned} F'_0 = & F_0 + \hat{\mathcal{D}}(\mathbb{1} - \hat{\Pi}) \hat{\mathcal{L}}_{\text{LD}} F_0 + \\ & + \hat{\mathcal{D}}(\mathbb{1} - \hat{\Pi}) \hat{\mathcal{L}}_{\text{LD}} [\hat{\Pi} + \hat{\mathcal{D}}(\mathbb{1} - \hat{\Pi})] \hat{\mathcal{L}}_{\text{LD}} F_0 + \dots, \end{aligned} \quad (25)$$

whereas in the redistribution models based on the Lambertian reflection, the expansions are written as:

$$\begin{aligned} F_{\text{out}} = & F_0 + [\hat{\Pi} + \hat{\mathcal{D}}(\mathbb{1} - \hat{\Pi})] \hat{\mathcal{L}}_{\text{LD}} F_0 \\ & + [\hat{\Pi} + \hat{\mathcal{D}}(\mathbb{1} - \hat{\Pi})] [\hat{\mathcal{L}}_{\text{LD}} \hat{\mathcal{D}}(\mathbb{1} - \hat{\Pi}) + \hat{\mathcal{L}}_0 \hat{\Pi}] \hat{\mathcal{L}}_{\text{LD}} F_0 + \dots, \end{aligned} \quad (26)$$

$$\begin{aligned} F'_0 = & F_0 + \hat{\mathcal{D}}(\mathbb{1} - \hat{\Pi}) \hat{\mathcal{L}}_{\text{LD}} F_0 \\ & + \hat{\mathcal{D}}(\mathbb{1} - \hat{\Pi}) [\hat{\mathcal{L}}_{\text{LD}} \hat{\mathcal{D}}(\mathbb{1} - \hat{\Pi}) + \hat{\mathcal{L}}_0 \hat{\Pi}] \hat{\mathcal{L}}_{\text{LD}} F_0 + \dots. \end{aligned} \quad (27)$$

By comparing the expressions for  $F_{\text{out}}$  ( $F'_0$ ) in different reflection approaches we see that they differ in underlined second order terms. The difference is typically small and likely not measurable at the current level of precision. However, it is conceptually important as it corresponds to a different physical description of the surface boundary energy balance.

#### 4.2. Lossy reflection-redistribution models

Energy is conserved when the difference between the total emitted flux  $L_{\text{out}}$  and the total incident flux  $L_{\text{in}}$  equals the total intrinsic flux  $L_0$ :

$$L_{\text{out}} - L_{\text{in}} = L_0 \quad L_* = \int_{\mathcal{M}} F_*(\mathbf{r})dA(\mathbf{r}), \quad \text{where } * = \text{out, in, } 0. \quad (28)$$

If we want to account for the processes that are not included in the energy balance (such as scattering), then the total flux per Eq. (14) is not conserved. The losses can occur at different levels:

- a) the decrease in the non-reflected part of the incident light at the surface of the irradiated star, described by the scalar function  $\xi(\mathbf{r}) \in [0, 1]$ :

$$\delta F_0 = \hat{\mathcal{D}}(1 - \hat{\Pi})\hat{\Xi}F_{\text{in}} \quad (29)$$

where we introduce auxiliary operator  $\hat{\Xi} : f \mapsto \xi f$  to describe the losses;

- b) the decrease of energy in the interior of the irradiated star, described by a “lossy” redistribution operator  $\hat{\mathcal{D}}'$ :

$$\delta F_0 = \hat{\mathcal{D}}'(\mathbb{1} - \hat{\Pi})F_{\text{in}}, \quad \int_{\mathcal{M}} [\hat{\mathcal{D}}'F](\mathbf{r})dA(\mathbf{r}) \leq \int_{\mathcal{M}} F(\mathbf{r})dA(\mathbf{r}); \quad \text{or} \quad (30)$$

- c) the decrease in emergent light at the surface of the radiating star, described analogously to case (a):

$$\delta F_0 = \hat{\Xi}\hat{\mathcal{D}}(\mathbb{1} - \hat{\Pi})F_{\text{in}}. \quad (31)$$

If the loss and reflection coefficients  $\xi$  and  $\rho$  are constant over the surface, we can express flux losses  $L_{\text{loss}} = L_0 - (L_{\text{out}} - L_{\text{in}})$  in the cases (a) and (b) as:

$$L_{\text{loss}} = L_{\text{in}}(1 - \rho)(1 - \xi),$$

where  $L_{\text{in}}$  can not be written in a simple form as it depends on the radiosity operators. Setting  $\xi = 1$  eliminates the losses. Flux conservation can be described by the three fractions, all with respect to the incident flux: the part of the incident flux reflected from the surface,  $R_{\text{refl}}$ ; the part of the flux absorbed and then redistributed across the surface,  $R_{\text{redistr}}$ ; and the part of the flux that is lost at the surface,  $R_{\text{lost}}$ :

$$R_{\text{refl}} + R_{\text{redistr}} + R_{\text{lost}} = 1, \quad (32)$$

where  $R_{\text{refl}} \equiv \rho$ ,  $R_{\text{redistr}} \equiv \xi(1 - \rho)$  and  $R_{\text{lost}} \equiv (1 - \xi)(1 - \rho)$ .

### 4.3. The definition of effective temperature

The effective temperature of a surface element is defined by the radiosity  $F$  of blackbody emission:

$$T_{\text{eff}}(\mathbf{r}) = \frac{1}{\sigma} F(\mathbf{r})^{\frac{1}{4}}, \quad (33)$$

where  $\sigma$  is the Stefan-Boltzmann constant. In the absence of reflection, the radiosity of a star equals the intrinsic exitance  $F_0$  and the corresponding intrinsic effective temperature is denoted by  $T_{\text{eff},0}$ . In the presence of reflection, the radiosity equals  $F_{\text{out}}$  as defined by the reflection models. It is always larger than  $F_0$ , so the effective temperature is also always larger than  $T_{\text{eff},0}$ :

$$T'_{\text{eff}}(\mathbf{r}) = T_{\text{eff},0}(\mathbf{r}) \left( \frac{F_{\text{out}}(\mathbf{r})}{F_0(\mathbf{r})} \right)^{\frac{1}{4}} = T_{\text{eff},0}(\mathbf{r}) \left( 1 + \rho(\mathbf{r}) \frac{F_{\text{in}}(\mathbf{r})}{F_0(\mathbf{r})} \right)^{\frac{1}{4}}. \quad (34)$$

## 5. DISCRETIZATION OF THE IRRADIATION FRAMEWORK

In order to use the presented irradiation framework in practice, all introduced operators, i.e., radiosity  $\hat{\mathcal{L}}_*$  ( $*$  = L, LD), reflection  $\hat{\Pi}$  and redistribution  $\hat{D}$ , and all function defined on the surface and describe physical properties of the body, such as radiosity, intensity and emittance, need to be discretized.

### 5.1. Basic concepts behind discretization

We start the discretization by partitioning the surface  $\mathcal{M}$  into distinct subsets:

$$\mathcal{M} = \bigcup_i \mathcal{S}_i \quad \mathcal{S}_i \cap \mathcal{S}_j = 0 \quad i \neq j. \quad (35)$$

with their area equal to

$$A_i = \int_{\mathcal{S}_i} dA(\mathbf{r}). \quad (36)$$

We approximate functions defined on surface as functions constant over any surface element  $\mathcal{S}_i$ , called piece-wise constant function over  $\mathcal{M}$ . A piece-wise constant approximation  $\tilde{f}$  of an integrable function  $f$  defined on the surface  $\mathcal{M}$  is given by

$$\tilde{f}(\mathbf{r}) = \sum_i f_i \chi_i(\mathbf{r}) \quad \chi_i(\mathbf{r}) = \begin{cases} 1 & : \mathbf{r} \in \mathcal{S}_i \\ 0 & : \text{otherwise} \end{cases}. \quad (37)$$

with expansion coefficients  $f_i$  expressed as

$$f_i = \frac{1}{A_i} \int_{\mathcal{S}_i} f(\mathbf{r}) dA(\mathbf{r}), \quad (38)$$

where  $\chi_i(\mathbf{r})$  is a characteristic function of  $\mathcal{S}_i$  on  $\mathcal{M}$ . The set  $\{\chi_i(\mathbf{r})\}$  is a functional basis of piece-wise constant functions. We treat vector  $\mathbf{f} = (f_i)$  as discretized version of function  $f$ .

Here considered operators are linear and therefore can be written in the form:

$$\hat{O}f(\mathbf{r}) = \int_{\mathcal{M}} H(\mathbf{r}, \mathbf{r}') f(\mathbf{r}') dA(\mathbf{r}'), \quad (39)$$

where  $H(\mathbf{r}, \mathbf{r}')$  is a kernel function that depends on the operator we are considering. Let us have a piece-wise constant function  $f = \sum_i f_i \chi_i$  with expansion coefficients  $f_i$ . We approximate its image  $\hat{O}f$  by a piece-wise constant function  $\sum_i f'_i \chi_i$  with the expansion coefficients given by

$$f'_i = \sum_j O_{i,j} f_j, \quad (40)$$

where the matrix elements  $O_{i,j}$  are expressed as

$$O_{i,j} = \frac{1}{A_i} \int_{\mathcal{S}_i} \int_{\mathcal{S}_j} H(\mathbf{r}, \mathbf{r}') dA(\mathbf{r}') dA(\mathbf{r}). \quad (41)$$

The matrix  $\mathbf{O} = [O_{i,j}]$  is the discretized version of the operator  $\hat{O}$ . In the case of the radiosity operator,  $O_{i,j}$  are the generalizations of the view-factors (Modest 2013). For the discretized version of the redistribution operator  $\hat{\mathbf{D}}$ , denoted by  $\mathbf{D} = [D_{i,j}]$ , the flux conservation takes the form:

$$\sum_i A_i D_{i,j} = A_j. \quad (42)$$

## 5.2. Calculations on the triangular surfaces and practical considerations

The irradiation framework is implemented by extending open-source package PHOEBE, where the working surface  $\mathcal{M}$  is a mesh of triangles that approximates the true shape of astrophysical bodies. We consider two discretization schemes for operators, per-triangle discretization and per-vertex discretization, as described in Prša et al. (2016). In both cases we simplify the expressions for matrix elements Eq. (41) to:

$$O_{i,j} \approx A_j H(\mathbf{r}_i, \mathbf{r}_j), \quad (43)$$

where  $\mathbf{r}_i$  and  $\mathbf{r}_j$  are surface element locations and  $A_i$  are the corresponding areas.

In the decomposition of the redistribution operators we need the distances across the surfaces. The calculation of distances on the triangular meshes is computationally very expensive, see e.g. Martínez et al. (2005). As astrophysical bodies are close to spherical, we can frequently approximate the distances by those on the sphere, which is computationally tractable. Consider our object of interest packed inside a sphere of radius  $R$  and center  $\mathbf{c}$ , satisfying:

$$\sum_i (\|\mathbf{r}_i - \mathbf{c}\|^2 - R^2)^2 = \min. \quad (44)$$

Next, define an operator to obtain the radial unit vector at a point on the sphere w.r.t. the center  $\mathbf{c}$ :

$$\hat{\mathbb{P}}\mathbf{r} = \frac{\mathbf{r} - \mathbf{c}}{\|\mathbf{r} - \mathbf{c}\|}. \quad (45)$$

The geodesic distance between the two points on the mesh,  $(\mathbf{r}_1, \mathbf{r}_2)$ , is approximated by the distance between the corresponding points on the sphere:

$$d(\mathbf{r}_1, \mathbf{r}_2) = R \arccos((\hat{\mathbb{P}}\mathbf{r}_1) \cdot (\hat{\mathbb{P}}\mathbf{r}_2)). \quad (46)$$

Furthermore, if the local curvature of the mesh is small, i.e. the mesh points are dense and the distances between neighbouring points considered for local redistribution do not differ much from the geodesic, we can approximate the distances with the Euclidean form:

$$d(\mathbf{r}_1, \mathbf{r}_2) \approx \|\mathbf{r}_1 - \mathbf{r}_2\|. \quad (47)$$

The deviation from the surface, measured along the axis  $\phi$ , ( $\|\phi\| = 1$ ), is then:

$$d_{\perp}(\mathbf{r}_1, \mathbf{r}_2) = R \arccos\left(\sqrt{(1 - u_1^2)(1 - u_2^2)} + u_1 u_2\right), \quad u_i = \phi \cdot \hat{\mathbb{P}}\mathbf{r}_i. \quad (48)$$

The local and latitudinal redistribution models, based on  $d$  and  $d_{\perp}$ , are schematically depicted in Fig. 2. The flux incident on the surface element centered on the vertex depicted in black is redistributed over the surface elements depicted in yellow, associated with the vertices depicted in red. The fraction of the incident flux that is redistributed over the elements depends on the weight function discussed before.

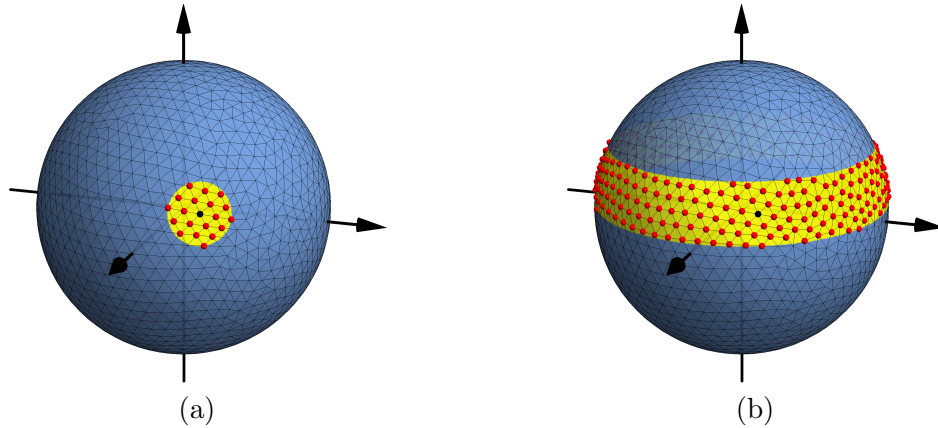


**Figure 2.** Schematic figure of the local (a) and latitudinal (b) redistribution of the flux incident on the surface element surrounding the vertex depicted in black and emitted from the surface elements that surround the vertices depicted in red.

### 5.3. Irradiation parameters

For most practical cases it suffices to assume discrete redistribution models (i.e. local, latitudinal and global) with constant reflection coefficients. Irradiation parameters  $\rho_{\text{refl}}$ ,  $\rho_{\text{local}}$ ,  $\rho_{\text{lat}}$  and  $\rho_{\text{uniform}}$  that are associated with the reflection and the local, latitudinal and uniform redistributions, respectively, are used to construct operator weights (cf. Eq. 17):

$$w_{\text{local}} = \frac{\rho_{\text{local}}}{1 - \rho_{\text{refl}}}, \quad w_{\text{lat}} = \frac{\rho_{\text{lat}}}{1 - \rho_{\text{refl}}}, \quad w_{\text{uniform}} = \frac{\rho_{\text{uniform}}}{1 - \rho_{\text{refl}}}, \quad (49)$$

which, in turn, determine the redistribution matrix for a given object:

$$\mathbf{D} = w_{\text{local}}\mathbf{D}_{\text{local}} + w_{\text{lat}}\mathbf{D}_{\text{lat}} + w_{\text{uniform}}\mathbf{D}_{\text{uniform}} . \quad (50)$$

The principal advantage of these irradiation parameters is that they add up to 1 for each body separately (assuming no losses), and each individual parameter represents the fraction of the total incoming flux redistributed by the given irradiation process.

#### 5.4. Solving discrete reflection-redistribution equations

We follow the presented discretization procedure and approximate all operators by matrices and all functions defined on the surface by vectors with their entries representing average quantities on surface elements. The discretized limb-darkened  $\hat{\mathcal{L}}_{\text{LD}}$  and Lambertian  $\hat{\mathcal{L}}_{\text{L}}$  radiosity operators are represented by matrices  $\mathbf{L}_{\text{LD}}$  and  $\mathbf{L}_{\text{L}}$ , respectively, and the redistribution operator  $\hat{\mathcal{D}}$  is described by matrix  $\mathbf{D}$  and the reflection operator  $\hat{\Pi}$  is approximated by  $\mathbf{\Pi}$ . The radiosity  $F_{\text{out}}$ , intrinsic exitance  $F_0$ , updated exitance  $F'_0$ , irradiation  $F_{\text{in}}$  are approximated by vectors  $\mathbf{F}_{\text{out}}$ ,  $\mathbf{F}_0$ ,  $\mathbf{F}'_0$  and  $\mathbf{F}_{\text{in}}$ , respectively.

The essential redistribution-reflection equations are given by Eq. (18) for Wilson's reflection and by Eq. (20) for the Lambertian reflection model. Following the discretization rules we can be written in matrix form as:

$$\mathbf{F}_{\text{out}} = \mathbf{G}_{\text{W}} + \mathbf{Q}_{\text{W}} \cdot \mathbf{F}_{\text{out}} \quad \text{for Wilson's model,} \quad (51)$$

$$\mathbf{F}_{\text{in}} = \mathbf{G}_{\text{L}} + \mathbf{Q}_{\text{L}} \cdot \mathbf{F}_{\text{in}} \quad \text{for Lambertian model,} \quad (52)$$

where we for the same of compact writing introduce auxiliary vectors  $\mathbf{G}_{\text{W}}$  and  $\mathbf{G}_{\text{L}}$  given by,

$$\mathbf{G}_{\text{L}} = \mathbf{F}_0 \quad \mathbf{G}_{\text{W}} = \mathbf{L}_{\text{LD}}\mathbf{F}_0 , \quad (53)$$

and matrices  $\mathbf{Q}_s$  written as,

$$\mathbf{Q}_{\text{W}} = [\mathbf{D}(\mathbf{1} - \mathbf{\Pi}) + \mathbf{\Pi}] \mathbf{L}_{\text{LD}} \quad \mathbf{Q}_{\text{L}} = \mathbf{L}_{\text{LD}}\mathbf{D}(\mathbf{1} - \mathbf{\Pi}) + \mathbf{L}_{\text{L}}\mathbf{\Pi} . \quad (54)$$

Vectors  $\mathbf{G}_{\text{W}}$  and  $\mathbf{G}_{\text{L}}$  represent intrinsic exitance and limb-darkened irradiated exitance, respectively, whereas matrices  $\mathbf{Q}_s$  represents the products of the discretized radiosity operator, reflection coefficients and the redistribution operator associated with a given reflection-redistribution scheme described by equations (18) and (20).

By design, the matrices  $\mathbf{Q}_s$  scales linearly with the discretized radiosity operators and, consequently, its norm is  $\leq 1$ . Because of that, Eqs. (51-52) are convergent and can be solved iteratively:

$$\mathbf{F}_{k+1} = \mathbf{G}_s + \mathbf{Q}_s \cdot \mathbf{F}_k \quad \text{for } k = 0, 1, \dots , \quad (55)$$

with  $s = \text{W, L}$  labeling the redistribution-reflection scheme and using the initial condition  $\mathbf{F}_0 = \mathbf{G}_s$ .

Note that the redistribution matrices  $\mathbf{D}_{\text{local}}$  and  $\mathbf{D}_{\text{lat}}$ , and the radiosity matrices  $\mathbf{L}_{\text{LD}}$  and  $\mathbf{L}_0$  are sparse matrices in all practical cases, and that the uniform redistribution matrix  $\mathbf{D}_{\text{uniform}}$  can be expressed as a projection:

$$\mathbf{D}_{\text{uniform}} = \frac{1}{A} [1, \dots, 1]^T [A_1, A_2, \dots], \quad (56)$$

where  $A = \sum_i A_i$ . These properties can significantly speed up the calculations.

Accurate irradiation calculations can be very time consuming as they involve solving a large sparse system of linear equations, as described in this section. Therefore, it is useful to have an approximate model to determine the magnitude of irradiation effects in order to decide whether they need to be taken into account given the required precision. We provide a detailed discussion in Appendix B.

## 6. DEMONSTRATION OF PRINCIPLES

In this section we demonstrate the irradiation models and underlying redistribution processes for several toy models to get a qualitative understanding of the presented irradiation models. To this end we use PHOEBE (Prša et al. 2016), an open source package for modeling eclipsing binaries, where we implement irradiation framework using discretized operator as presented in Section 5.

### 6.1. Irradiance and radiosity in a two-sphere system

Consider a system of two identical spheres with a constant exitance  $F_0$ . The consequence of mutual irradiation is the updated exitance  $F'_0$  and radiosity  $F$  of the two spheres. We compute it by using Lambertian reflection and a specific redistribution model with a linear weight function  $g(x) = 1 - x/l$ . The results are depicted in Fig. 3 as a density plot of  $F'_0$  and  $F$  across the surfaces of the spheres. Common to all redistribution models is that the increase of the reflection coefficient decreases the incident flux redistributed over the surface and, in consequence, a decrease in  $F'_0$ ; and the increase of the area over which the incoming flux is redistributed makes  $F'_0$  more uniform across the surface and, on average, decreased in size.

In order to highlight the effects of both processes, reflection and redistribution, we choose a reflection coefficient  $\rho = 0.3$ , which is large enough to have notable reflection and small enough to enable significant redistribution. Fig. 3 shows that the uniform redistribution produces a uniform  $F'_0$  and represents a bias value for radiosity, as indicated by Eq. (13); the local redistribution generally gives the largest  $F'_0$  and  $F$ , and both distributions have a similar shape; and lastly, the latitudinal redistribution increases exitance at latitudes that are most strongly illuminated.

An mean-field approximation of here discussed two-sphere case with a focus on average radiosity and irradiance is presented in Appendix B and can be used to check the order of magnitude of reflection-redistribution effects.

### 6.2. Detecting and discriminating redistribution effects

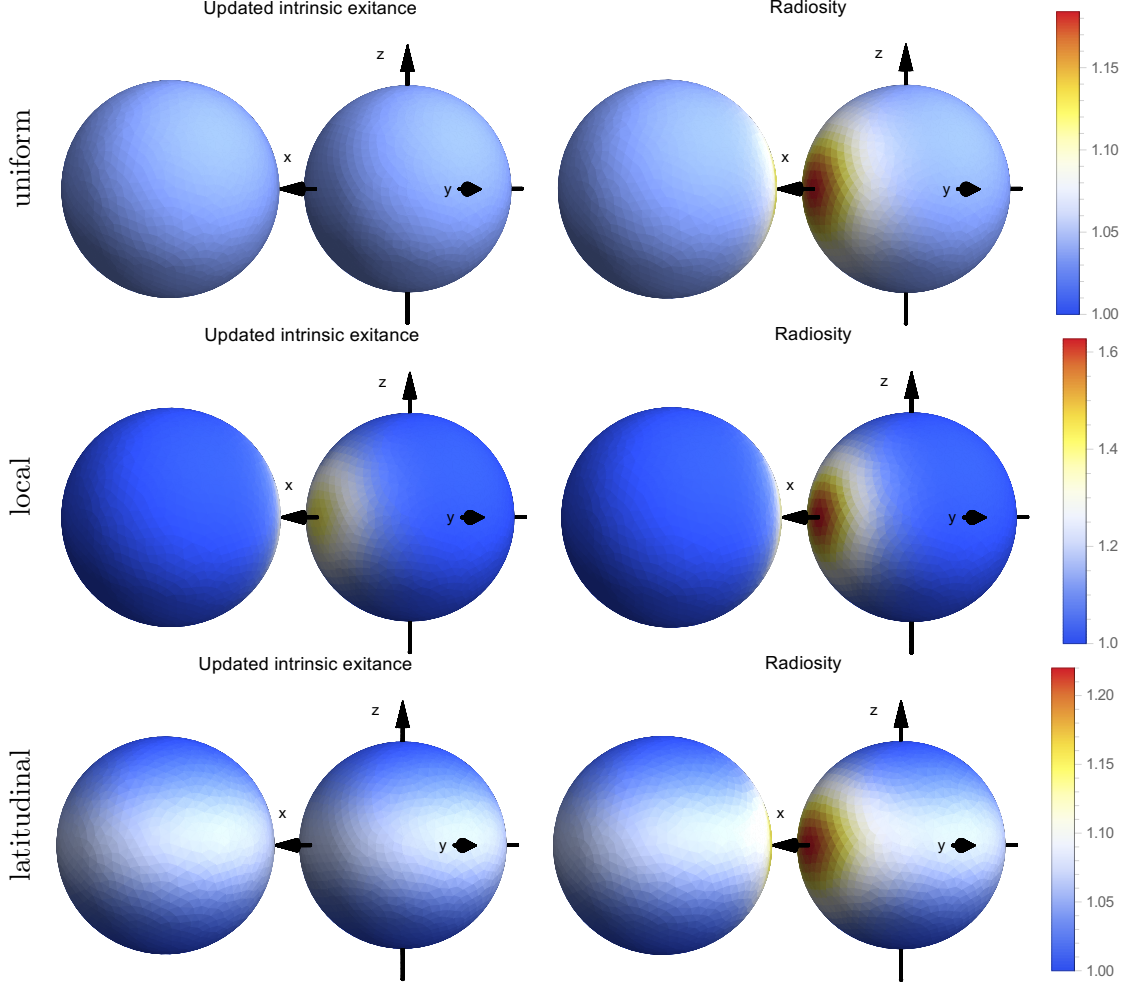


**Figure 3.** The changes in updated radiance and radiosity as a function of redistribution model. Each row corresponds to a specific redistribution type for a system of two spherical stars. Both stars have a relative size  $R = 1$  and the centers of the stars are separated by  $L = 2.5$ . The Lambertian reflection approach has been implemented with reflection and linear limb-darkening coefficients of  $\rho = 0.3$  and  $x = 0.3$ , respectively. The intrinsic emission for both stars is set to  $F_0 = 1$  and we use a linear weight function  $g$  with the threshold value of  $l/R = 0.2$ .

We apply the introduced irradiation models by calculating light curves for a binary star with redistribution switched both on and off. We consider simplified reflection in which reflection coefficients are constant across a body. In addition, we discuss how well we can discriminate between different redistribution effects based on the light curves.

Consider a model light curve (LC) with certain redistribution parameters  $\mathbf{x} \in \mathbb{R}^p$  calculated at  $N$  timestamps:  $\mathbf{C}(\mathbf{x}) = [C_i(\mathbf{x})]_{i=1}^N \in \mathbb{R}^N$ . In the vicinity of parameters  $\mathbf{x}$  (i.e. for perturbed parameters  $\mathbf{x}' = \mathbf{x} + \delta\mathbf{x} \in \mathbb{R}^p$ ) we can approximate this LC vector by its Taylor expansion:

$$\mathbf{C}(\mathbf{x}') = \mathbf{C}(\mathbf{x}) + \mathbf{C}'(\mathbf{x})\delta\mathbf{x} + \mathcal{O}(\|\delta\mathbf{x}\|^2).$$



The vector norms here in use are denoted by  $\|\cdot\|$  and for a vector  $\mathbf{x}$  is defined as  $\|\mathbf{x}\| = \sqrt{\mathbf{x}^T \mathbf{x}}$ . The discrepancy between the LC vector at parameters  $\mathbf{x}$  and at the perturbed parameters  $\mathbf{x}'$  is measured by the norm of the difference of LC vectors, written as:

$$\|\mathbf{C}(\mathbf{x}') - \mathbf{C}(\mathbf{x})\|^2 = \delta \mathbf{x}^T \mathbf{C}'^T(\mathbf{x}) \mathbf{C}'(\mathbf{x}) \delta \mathbf{x} + \mathcal{O}(\|\delta \mathbf{x}\|^3). \quad (57)$$

The discrepancy can be quantified by performing a singular value decomposition (SVD) of the LC vector derivative:

$$\mathbf{C}'(\mathbf{x}) = \mathbf{U}(\mathbf{x}) \mathbf{\Sigma}(\mathbf{x}) \mathbf{V}^T(\mathbf{x}), \quad (58)$$

where  $\mathbf{U}(\mathbf{x}) \in \mathbb{R}^{N \times N}$  and  $\mathbf{V}(\mathbf{x}) \in \mathbb{R}^{p \times p}$  are orthogonal matrices and  $\mathbf{\Sigma}(\mathbf{x}) \in \mathbb{R}^{N \times p}$  is a diagonal matrix with singular values on the diagonal: the maximal and the minimal value on the diagonal are  $\sigma_{\max}$  and  $\sigma_{\min}$ , respectively. For detail on SVD see, e.g., Širca & Horvat (2018), The discrepancy of the LC vector in the limit of small perturbations is then bound by the singular values:

$$\sigma_{\min}(\mathbf{x}) \|\delta \mathbf{x}\| \leq \|\mathbf{C}(\mathbf{x} + \delta \mathbf{x}) - \mathbf{C}(\mathbf{x})\| \leq \sigma_{\max}(\mathbf{x}) \|\delta \mathbf{x}\|. \quad (59)$$

When  $\sigma_{\min}$  is zero, there is a linear combination of irradiation effects that do not produce changes in the light curve, resulting in a degenerate case. Note that  $\sigma_{\min}$  and  $\sigma_{\max}$  have a dimension and, consequently, they scale linearly with the amplitude of the light curve.

Typically the difference in light curves  $\mathbf{C}(\mathbf{x} + \delta \mathbf{x}) - \mathbf{C}(\mathbf{x})$  can be measured up to a certain noise level. Let us denote the discrepancy between measured and computed light curve as  $\mathbf{N}$  and treat it as noise<sup>2</sup>. The changes in irradiation parameters  $\delta \mathbf{x}$  are detectable if:

$$\|\delta \mathbf{x}\| \geq \frac{\|\mathbf{N}\|}{\sigma_{\max}(\mathbf{x})} \equiv \epsilon_{\text{sufficient}} \quad (60)$$

and all changes in irradiation parameters are measurable if:

$$\|\delta \mathbf{x}\| \geq \frac{\|\mathbf{N}\|}{\sigma_{\min}(\mathbf{x})} \equiv \epsilon_{\text{total}}. \quad (61)$$

To quantify how well we can discriminate between effects, we need to consider how strongly the light curve varies due to changes in irradiation parameters about  $\mathbf{x}$ . We quantify the variation by the ratio between the largest and the smallest response in the light-curve vector equal to the condition number (Širca & Horvat 2018):

$$\kappa(\mathbf{x}) = \frac{\epsilon_{\text{total}}}{\epsilon_{\text{sufficient}}} = \frac{\sigma_{\max}(\mathbf{x})}{\sigma_{\min}(\mathbf{x})} \geq 1. \quad (62)$$

In order to clearly separate the effect of different parameters on the light-curve,  $\kappa$  needs to be as large as possible and  $\|\delta \mathbf{x}\| \geq \epsilon_{\text{total}}$ . Note that, in the degenerate case, the conditional number  $\kappa$  is infinite and so is  $\epsilon_{\text{total}}$ .

<sup>2</sup> If the noise is uncorrelated with standard deviation  $\sigma_{\text{noise}}$ , the statistical averages of the vector norm of the noise and the corresponding square are  $\langle \|\mathbf{N}\| \rangle = \sqrt{\frac{2N}{\pi}} \sigma_{\text{noise}}$  and  $\langle \|\mathbf{N}\|^2 \rangle = N \sigma_{\text{noise}}^2$ , respectively.

### 6.3. Bolometric light curves for a toy binary system

We are studying irradiation effects in a toy binary system motivated by NN Serpentis, an eclipsing binary system composed of a white dwarf and red dwarf with an orbital period of 0.13 days (Qian et al. 2009; Parsons et al. 2010), although without its recently discovered circumbinary disc (Hardy et al. 2016). The parameters of toy system are listed in Table 1. The synthetic bolometric light curves and radial velocity curves are calculated in the limiting cases, i.e. the absence of redistribution; the presence of only local redistribution; the presence of only latitudinal redistribution; and the presence of only uniform redistribution.

**Table 1.** Parameters for NN Serpentis-like system based on data in Parsons et al. (2010).

Parameter	white dwarf	red dwarf
atmosphere	blackbody	blackbody
exponent in gravity brightening $g$	1	0.32
polar radius $R[R_{\odot}]$	0.0211	0.147
effective temperature $T_{\text{eff}}[K]$	57000	3500
masses $M[M_{\odot}]$	0.535	0.111
fraction of reflection $\rho_{\text{refl}}$	1	0.6
limb darkening (LD):		
model	logarithmic	logarithmic
coefficient $x_{\text{LD}}$	0.5	0.5
coefficient $y_{\text{LD}}$	0.5	0.5
orbit:		
period $P[\text{d}]$	0.1300801714	
eccentricity $\epsilon$	0	
systemic velocity $\gamma[\text{km/s}]$	0	
inclination $\iota[\text{deg}]$	89.6	
mass ratio $M_2/M_1$	0.207	
semi-major axis $a[R_{\odot}]$	0.934	

We assume that the albedos (i.e. fraction of the flux that is reflected directly from the surface) of the primary and secondary stars are  $\rho_{\text{P}} = 1$  and  $\rho_{\text{S}} = 0.6$ , respectively, and that the radii of the latitudinal and local redistribution processes for both bodies are  $l/R = 20^{\circ}$ . The light curves and radial velocity curves of such a system are presented in Fig. 4.

The redistribution increases the emitted flux. The strongest increase is noticeable with local redistribution, as we can see from Fig. 4a. This is because it effectively increases the reflectivity of the object, resulting in an increased radiosity/fluxes at times for which already expect strong reflection contributions with its peak at the secondary eclipse. The latitudinal and uniform redistribution have a similar effect on the light curve, but because the uniform redistribution spreads the incoming flux over a wider area (the whole body) than the latitudinal redistribution, the flux of the former case is necessarily smaller than the flux of the latter case.

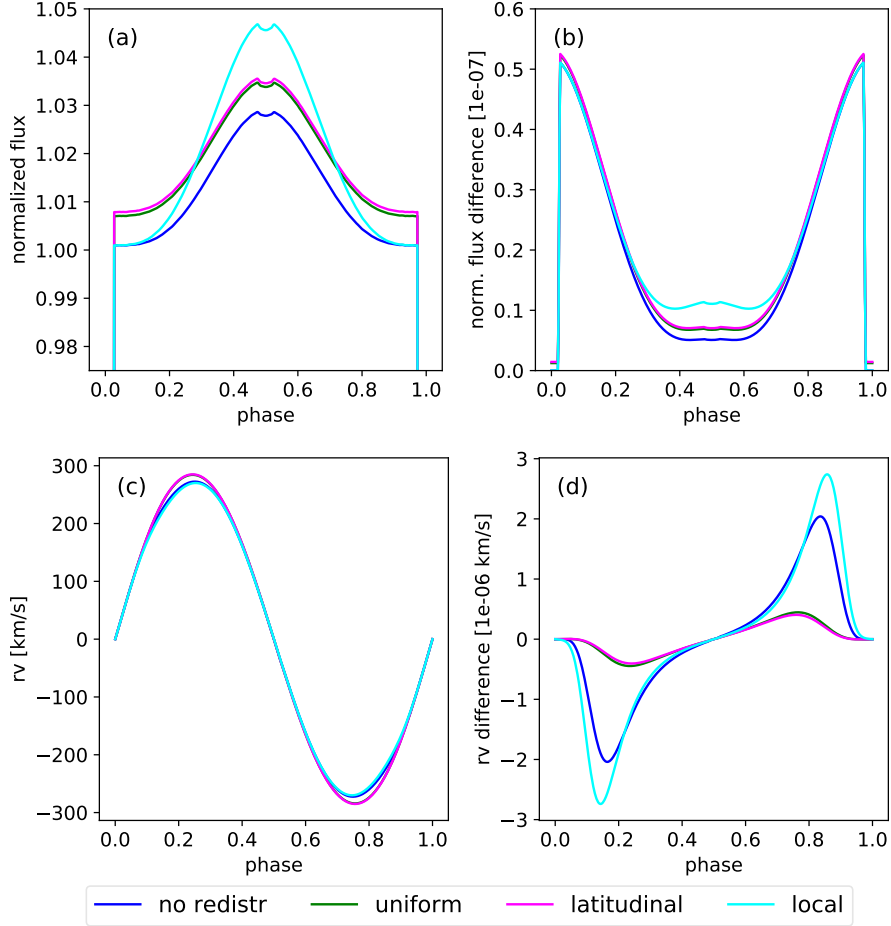


**Figure 4.** The computed light curve (top row) and radial velocity curves (bottom row) of a NN Serpentis-like system using Lambertian reflection with different redistribution schemes (left column) and the difference between the curves obtained using the Lambertian scheme and Wilson’s reflection approach (right column). The models are normalized such that the bolometric luminosity (prior to any irradiation effects) of the primary component is kept fixed at  $4\pi$  between different models, such that, in isolation, it would effectively contribute unity to the overall flux. As the secondary component is much less luminous, the majority of additional flux is from the irradiation on the secondary component by the primary, which differs between these different schemes.

The redistribution does affect radial velocities as strongly as fluxes, see Fig. 4c. Interestingly, we obtain a similar radial velocity curves for pairs of latitudinal and uniform redistribution, and local and no redistribution. This is a consequence that the local redistribution affects only a small area on the surface in comparison to the uniform and latitudinal redistribution.

Differences between the Wilson and Lambertian reflection schemes in light curves and radial velocities are of the order of magnitude  $10^{-7}$  and  $10^{-8}$  and presented in Fig. 4b and Fig. 4c, respectively. Currently, these differences are not measurable in practice. The fluxes obtained using Wilson’s approach are larger than using Lambertian reflection, which seems to be generally true in a binary configuration. This follows from the fact that limb-darkened (Wilson) diffusion of light amplifies the in-

tensities in the direction nearly normal to the surface in comparison to Lambertian diffusion, where  $D/D_0 > 1/\pi$  for  $\mu \approx 1$  for almost all limb-darkening coefficients. The intensities in the direction nearly orthogonal to the surface are the most important in the transfer of energy between the bodies, yielding an increase in reflected fluxes and consequently an increase in radiosity. The differences between radial velocity curves obtained using Wilson or Lambertian reflection and some redistribution type are pair-wise similar in shape for the local and without redistribution and the uniform and latitudinal redistribution. The differences of the latter pair are generally smaller, because the redistribution to a wider area has an effect of blurring out local differences in radiosity across the lobe.

Following the analysis presented in Sec. 6.2 we calculate  $\sigma_{\max}$  and  $\sigma_{\min}$  by varying redistribution parameters of the second star for the cases discussed in Fig. 4 and find that  $\sigma_{\max} \approx 0.48$ ,  $\sigma_{\min} = 0.00285$  and resulting conditional number  $\kappa \approx 169$  (Eq. 62) This suggests that these cases are far from degenerate and according to Eq. (59) the effect of the redistribution in the light curve can vary by up to two-orders in magnitude, at the same magnitude of redistribution parameters

## 7. CONCLUSIONS

In this paper we present a general framework for dealing with quasi-stationary irradiation effects between astrophysical bodies. It extends the reflection schemes presented in Prša et al. (2016) to include redistribution, thereby making the framework energy conserving. This framework can essentially be used to describe any arbitrary pattern of redistribution, but here we focus on three possible redistribution processes for nearly spherical bodies, where we can at least partially justify the functional form of redistribution operators.

We have demonstrated the framework on a toy binary system resembling NN Serpentis in order to confirm that a significant part of the irradiation is absorbed, and therefore that the redistribution effect should be a noticeable. In the considered case, the difference between reflection schemes are very small and not measurable at the current best precision of observational measurements.

As highlighted by Wilson (1990), a “complete” treatment of the irradiation effect can be broken into four main components: geometrical, bolometric energy exchange, irradiated stellar atmospheres, and induced changes to envelope structure. The framework presented here accurately treats the first two parts exactly and, importantly, with the inclusion of true energy conservation<sup>3</sup>. The final two aspects are clearly intertwined and highly dependent upon the system parameters, making their accurate treatment computationally expensive and somewhat impractical when attempting to model real-world systems. As such, the framework presented here represents the most comprehensive treatment of irradiation in binary stars to-date.

<sup>3</sup> Some fraction of the energy may contribute to changes in the structure of the irradiated stellar envelope, however our treatment assumes that this is a quasi-stable effect and thus the energy balance comprises only reflection and redistribution (with no additional fraction altering the envelope structure).

Beyond the clear open questions about the impact of irradiation on the stellar atmospheres and structures (and, more generally, on the validity of continuing to use non-irradiated models as representative of irradiated binary stars), there are several aspects of the redistribution and reflection processes which are far from being understood. Reflection is essentially characterized completely by the bolometric albedo, with theoretical considerations predicting a strong dependence on stellar effective temperature which has yet to be confirmed by observations (see, e.g.; Claret 2001). Redistribution is even more poorly understood with very few theoretical constraints available. For example, it is particularly unclear which (if any) of the functions (uniform, local, latitudinal) presented in this work is the most physical way of describing the redistribution process. Furthermore, in close systems where the components are gravitationally distorted, how is the redistribution process affected by such deviations from sphericity. PHOEBE, combined with the extended framework presented here, currently represents the most complete modelling tool with which to address these open questions observationally.

This work was supported by the NSF AAG grant #1517474, which we gratefully acknowledge. This research has been supported by the Spanish Ministry of Economy and Competitiveness (MINECO) under the grant AYA2017-83383-P.

## REFERENCES

- Barclay, T., Endl, M., Huber, D., et al. 2015, *The Astrophysical Journal*, 800, 46, doi: [10.1088/0004-637X/800/1/46](https://doi.org/10.1088/0004-637X/800/1/46)
- Barclay, T., Huber, D., Rowe, J. F., et al. 2012, *ApJ*, 761, 53, doi: [10.1088/0004-637X/761/1/53](https://doi.org/10.1088/0004-637X/761/1/53)
- Budaj, J. 2011, *The Astronomical Journal*, 141, 59, doi: [10.1088/0004-6256/141/2/59](https://doi.org/10.1088/0004-6256/141/2/59)
- Budaj, J., & Richards, M. T. 2004, *Contributions of the Astronomical Observatory Skalnaté Pleso*, 34, 167
- Claret, A. 2001, *MNRAS*, 327, 989, doi: [10.1046/j.1365-8711.2001.04783.x](https://doi.org/10.1046/j.1365-8711.2001.04783.x)
- . 2007, *A&A*, 470, 1099, doi: [10.1051/0004-6361:20077296](https://doi.org/10.1051/0004-6361:20077296)
- Cohen, M. F., & Wallace, J. R. 2016, *Radiosity and Realistic Image Synthesis* (San Francisco, CA, USA: Morgan Kaufmann Publishers Inc.)
- Gershbein, R., Schröder, P., & Hanrahan, P. 1994, in *Proceedings of the 21st Annual Conference on Computer Graphics and Interactive Techniques, SIGGRAPH '94* (New York, NY, USA: ACM), 51–58. <http://doi.acm.org/10.1145/192161.192171>
- Hapke, B. 2012, *Theory of Reflectance and Emittance Spectroscopy*, 2nd edn. (Cambridge University Press), doi: [10.1017/CBO9781139025683](https://doi.org/10.1017/CBO9781139025683)
- Hardy, A., Schreiber, M. R., Parsons, S. G., et al. 2016, *MNRAS*, 459, 4518, doi: [10.1093/mnras/stw976](https://doi.org/10.1093/mnras/stw976)
- Hubeny, I., Burrows, A., & Sudarsky, D. 2003, *ApJ*, 594, 1011, doi: [10.1086/377080](https://doi.org/10.1086/377080)
- Kallrath, J., & Milone, E. F. 2009, *Eclipsing Binary Stars: Modeling and Analysis - Astronomy and Astrophysics Library*, 2nd edn. (Springer Publishing Company, Incorporated), doi: [10.1007/978-1-4419-0699-1](https://doi.org/10.1007/978-1-4419-0699-1)

- Mandel, K., & Agol, E. 2002, *The Astrophysical Journal Letters*, 580, L171, doi: [10.1086/345520](https://doi.org/10.1086/345520)
- Martínez, D., Velho, L., & Carvalho, P. C. 2005, *Comput. Graph.*, 29, 667, doi: [10.1016/j.cag.2005.08.003](https://doi.org/10.1016/j.cag.2005.08.003)
- Modest, M. 2013, *Radiative Heat Transfer*, 3rd edn. (Academic Press), 904, doi: [10.1016/C2010-0-65874-3](https://doi.org/10.1016/C2010-0-65874-3)
- Nordlund, A., & Vaz, L. P. R. 1990, *A&A*, 228, 231
- Parsons, S. G., Marsh, T. R., Copperwheat, C. M., et al. 2010, *Monthly Notices of the Royal Astronomical Society*, 407, 2362, doi: [10.1111/j.1365-2966.2010.17063.x](https://doi.org/10.1111/j.1365-2966.2010.17063.x)
- Prša, A., & Zwitter, T. 2005, *ApJ*, 628, 426, doi: [10.1086/430591](https://doi.org/10.1086/430591)
- Prša, A., Harmanec, P., Torres, G., et al. 2016, *AJ*, 152, 41, doi: [10.3847/0004-6256/152/2/41](https://doi.org/10.3847/0004-6256/152/2/41)
- Prša, A., Conroy, K. E., Horvat, M., et al. 2016, *The Astrophysical Journal Supplement Series*, 227, 29, doi: [10.3847/1538-4365/227/2/29](https://doi.org/10.3847/1538-4365/227/2/29)
- Qian, S.-B., Dai, Z.-B., Liao, W.-P., et al. 2009, *The Astrophysical Journal Letters*, 706, L96, doi: [10.1088/0004-637X/706/1/L96](https://doi.org/10.1088/0004-637X/706/1/L96)
- Ruciński, S. M. 1969, *AcA*, 19, 245
- Širca, S., & Horvat, M. 2018, *Computational Methods in Physics: Compendium for Students, Graduate Texts in Physics* (Springer International Publishing), doi: [10.1007/978-3-319-78619-3](https://doi.org/10.1007/978-3-319-78619-3)
- Vaz, L. P. R., & Nordlund, A. 1985, *A&A*, 147, 281
- Wilson, R. E. 1990, *ApJ*, 356, 613, doi: [10.1086/168867](https://doi.org/10.1086/168867)

## APPENDIX

## A. RADIOSITY EQUATIONS IN INTEGRAL FORM

To better illustrate the principles, let us write out the reflection model equations in the integral form for two convex bodies, labeled as A and B, with the corresponding surfaces  $\mathcal{M}_A$  and  $\mathcal{M}_B$ . The irradiation operator can be written as:

$$\hat{Q}F(\mathbf{r}) = \int_{\mathcal{M}} Q(\mathbf{r}, \mathbf{r}') F(\mathbf{r}') dA(\mathbf{r}') .$$

The radiosity equation for [Wilson's](#) model, Eq. (9), for a point  $\mathbf{r}_B$  on the surface of star  $B$  can be written as:

$$F_{\text{out}}(\mathbf{r}_B) = F_0(\mathbf{r}_B) + \rho(\mathbf{r}_B) \int_{\mathcal{M}_A} Q(\mathbf{r}_B, \mathbf{r}_A) \frac{D(\widehat{(\mathbf{r}_B - \mathbf{r}_A)} \cdot \hat{\mathbf{n}}(\mathbf{r}_A))}{D_0(\mathbf{r}_A)} F_{\text{out}}(\mathbf{r}_A) dA(\mathbf{r}_A) .$$

This is equivalent to the relation given in [Wilson \(1990\)](#), except that it uses radiosity  $F_{\text{out}}$  instead of the flux density excess due to reflection,  $F_{\text{out}}/F_0$ .

The irradiance  $F_{\text{in}}$  for [Prša et al.'s](#) reflection model, Eq. (10), at  $\mathbf{r}_B$  on the surface of star  $B$  in integral form is:

$$F_{\text{in}}(\mathbf{r}_B) = \int_{\mathcal{M}_A} Q(\mathbf{r}_B, \mathbf{r}_A) \left[ \frac{D(\widehat{(\mathbf{r}_B - \mathbf{r}_A)} \cdot \hat{\mathbf{n}}(\mathbf{r}_A))}{D_0(\mathbf{r}_A)} F_0(\mathbf{r}_A) + \rho(\mathbf{r}_A) \frac{F_{\text{in}}(\mathbf{r}_A)}{\pi} \right] dA(\mathbf{r}_A) .$$

## B. IRRADIATION APPROXIMATION IN A TWO-BODY SYSTEM

Here we are providing a highly simplified model of irradiation for a binary system. In this model we reduce the bodies to points with a night and day side and make a rough estimate of the flux exchange on a line (from here comes the name one-dimensional) between day sides via irradiation and of redistribution between day and night side. The approximation is based on approximating average response of operator using the mean-field approach.

B.1. *The mean-field approximation*

All operators introduced in this paper, i.e reflection  $\hat{\Pi}$ , redistribution  $\hat{D}$  and radiosity  $\hat{\mathcal{L}}_*$  ( $*$  = L, LD) operators, preserve positivity of functions and all functions describing irradiation process, i.e. irradiance  $F_{\text{in}}$ , radiosity  $F_{\text{out}}$ , exitances  $F_0$  and  $F'_0$  are defined on the surfaces of bodies and non-negative.

In the mean-field approximation approach we decompose a function  $F$  defined on surface  $\mathcal{S}$  of area  $A$  into its surface average  $\langle F \rangle$ , defined as

$$\langle F \rangle = \frac{1}{A} \int F(\mathbf{r}) dA(\mathbf{r})$$

and deviation  $\delta F$  from it, writing  $F = \langle F \rangle + \delta F$ . Then an action of some operator  $\hat{O}$  on function  $F$  reads

$$\hat{O}F = \hat{O}\langle F \rangle + \hat{O}\delta F .$$

For here used operators and functions the first term on right is the dominant contribution. In the mean-field approximation we drop the term depending on fluctuations and approximate the surface average of operator image of an function as

$$\langle \hat{\mathcal{O}}F \rangle \approx \langle F \rangle \langle \hat{\mathcal{O}} \rangle \quad \text{and} \quad \langle \hat{\mathcal{O}} \rangle \equiv \langle \hat{\mathcal{O}}1 \rangle .$$

We call  $\langle \hat{\mathcal{O}} \rangle$  the average operator and is defined as an surface average of the image of the unity.

### B.2. One-dimensional model of irradiation

Let us discuss a system of two convex bodies, labeled as A and B, with the Lambertian reflection from the surfaces and introduce intrinsic exitances  $F_{0,b}$ , updated intrinsic exitances  $F'_{0,b}$ , exiting  $F_{\text{out},b}$  and entering  $F_{\text{in},b}$  radiosities defined for both bodies  $b = A, B$ . The updated intrinsic exitances  $F'_{0,b}$  and exiting radiosities  $F_{\text{out},b}$  are expressed as

$$F'_{0,b} = F_{0,b} + \hat{\mathcal{D}}_b(1 - \hat{\Pi}_b)F_{\text{in},b} \quad \text{and} \quad F_{\text{out},b} = F'_{0,b} + \hat{\Pi}_b F_{\text{in},b} , \quad (\text{B1})$$

where  $\hat{\mathcal{D}}_b$  and  $\hat{\Pi}_b$  are the redistribution operator and the reflection operators associated with body  $b$ , respectively. Consequently, we can separate the irradiation Eq. (20) into a system of two equations, each dealing with the irradiation of considered star:

$$F_{\text{in},B} = \hat{\mathcal{L}}_{\text{LD},A \rightarrow B} F_{0,A} + \left[ \hat{\mathcal{L}}_{\text{LD},A \rightarrow B} \hat{\mathcal{D}}_A (1 - \hat{\Pi}_A) + \hat{\mathcal{L}}_{\text{L},A \rightarrow B} \hat{\Pi}_A \right] F_{\text{in},A} , \quad (\text{B2})$$

$$F_{\text{in},A} = \hat{\mathcal{L}}_{\text{LD},B \rightarrow A} F_{0,B} + \left[ \hat{\mathcal{L}}_{\text{LD},B \rightarrow A} \hat{\mathcal{D}}_B (1 - \hat{\Pi}_B) + \hat{\mathcal{L}}_{\text{L},B \rightarrow A} \hat{\Pi}_B \right] F_{\text{in},B} . \quad (\text{B3})$$

The radiosity operators  $\hat{\mathcal{L}}_{\text{LD},b \rightarrow b'}$  and  $\hat{\mathcal{L}}_{\text{L},b \rightarrow b'}$  describe limb-darkened and Lambertian diffusion of light from the surface of body  $b$  onto the surface of body  $b'$ . For simplicity sake we assume a constant reflection on both bodies ( $b = A, B$ ):

$$\hat{\Pi}_b = \rho_b \mathbb{1}, \quad \rho_b = \text{const} .$$

The surface of the bodies can be divided into illuminated part, called day side, and non-illuminated part, called night side. The irradiation equations (B2) - (B3) describe processes only on the day side and consequently,  $F_{\text{in},b}$  is non-zero only on that side of body  $b = A, B$ . Additionally, we may notice that

$$F_{\text{out},b}(\mathbf{r}) = F'_{0,b}(\mathbf{r}) + \hat{\Pi}_b F_{\text{in},b}(\mathbf{r}) \quad \mathbf{r} \in \text{day side} , \quad (\text{B4})$$

$$F_{\text{out},b}(\mathbf{r}) = F'_{0,b}(\mathbf{r}) \quad \mathbf{r} \in \text{night side} . \quad (\text{B5})$$

Next we introduce the averages over the whole surface  $\langle \cdot \rangle$ , over the day side  $\langle \cdot \rangle_{\text{day}}$  and over the night side  $\langle \cdot \rangle_{\text{night}}$  of a considered body. The areas of entire surface and



of the day side of body  $b$  are denoted by  $A_b$  and  $A_{b,\text{day}}$ , respectively. Taking into account Eq. (B5) we can conclude for body  $b$  that

$$\langle F_{\text{out},b} \rangle = p \langle F_{\text{out},b} \rangle_{\text{day}} + (1-p) \langle F'_{0,b} \rangle_{\text{night}}, \quad (\text{B6})$$

where use the ratio of areas  $p = A_{b,\text{day}}/A_b$ .

We start the approximation of the irradiation model by decomposing all involved quantities, i.e.,  $F_{0,b}$ ,  $F'_{0,b}$  and  $F_{\text{out},b}$ , into their day and night side counterparts. Then take the surface average of irradiation Eqs. (B2)-(B3) and the quantities over the both sides of bodies separately. The irradiation equations are only defined on the day sides and so the night side averages yields zero. We approximate the actions of operators using a mean-field approach, whereby we replace functions defined across the day and night sides with their corresponding average, for details see Sec. B.1. Following this idea, we approximate the averages of operators acting on a function  $F$  defined over the day side of body  $b$  according to the next rules:

$$\langle \hat{\mathcal{L}}_{l,b \rightarrow b'} F \rangle_{\text{day}} \approx L_{l,b \rightarrow b'} \langle F \rangle_{\text{day}}, \quad (\text{B7})$$

$$\langle \hat{\mathcal{D}}_b F \rangle_{\text{day}} \approx \eta_b \langle F \rangle_{\text{day}}, \quad (\text{B8})$$

$$\langle \hat{\mathcal{D}}_b F \rangle_{\text{night}} \approx (1 - \eta_b) \langle F \rangle_{\text{day}}, \quad (\text{B9})$$

where  $l = \text{LD}, \text{L}$  is labelling different surface behavior. Here we introduce model constants  $L_{l,b \rightarrow b'}$  and  $\eta_b$  that describe the effective action of radiosity and redistribution operators on the surface-averaged incoming radiosity  $\langle F_{\text{in},b} \rangle_{\text{day}}$ . More precisely,  $L_{l,b \rightarrow b'}$  represents the average ratio of emitted energy transferred from points on body  $b$  to body  $b'$ , and  $\eta_b$  quantifies the average ratio of absorbed energy that is re-emitted on the same side.

The averages of quantities describing irradiation process over the day and night side are then given by

$$\langle F'_{0,b} \rangle_{\text{day}} = \langle F_{0,b} \rangle_{\text{day}} + (1 - \rho_b) \eta_b \langle F_{\text{in},b} \rangle_{\text{day}}, \quad (\text{B10})$$

$$\langle F'_{0,b} \rangle_{\text{night}} = \langle F_{0,b} \rangle_{\text{night}} + (1 - \rho_b) (1 - \eta_b) \langle F_{\text{in},b} \rangle_{\text{day}}, \quad (\text{B11})$$

$$\langle F_{\text{out},b} \rangle_{\text{day}} = \langle F'_{0,b} \rangle_{\text{day}} + \rho_b \langle F_{\text{in},b} \rangle_{\text{day}}, \quad (\text{B12})$$

$$\langle F_{\text{out},b} \rangle_{\text{night}} = \langle F'_{0,b} \rangle_{\text{night}}. \quad (\text{B13})$$

By introducing additional auxiliary coefficients

$$T_{b \rightarrow b'} = (1 - \rho_b) \eta_b L_{\text{LD},b \rightarrow b'} + \rho_b L_{\text{L},b \rightarrow b'}, \quad (\text{B14})$$

$$G_{b'} = L_{\text{LD},b \rightarrow b'} \langle F_{0,b} \rangle_{\text{day}}, \quad (\text{B15})$$

the averaged of irradiation equations (B2)-(B3) can be rewritten into a simple system of two scalar equations involving variables  $\langle F_{\text{in},b} \rangle_{\text{day}}$  for body  $b = A, B$ :

$$\langle F_{\text{in},A} \rangle_{\text{day}} = G_A + T_{B \rightarrow A} \langle F_{\text{in},B} \rangle_{\text{day}}, \quad (\text{B16})$$

$$\langle F_{\text{in},B} \rangle_{\text{day}} = G_B + T_{B \rightarrow A} \langle F_{\text{in},B} \rangle_{\text{day}}. \quad (\text{B17})$$

The solution of this system is equal to

$$\begin{bmatrix} \langle F_{\text{in,A}} \rangle_{\text{day}} \\ \langle F_{\text{in,B}} \rangle_{\text{day}} \end{bmatrix} = \frac{1}{1 - T_{\text{B} \rightarrow \text{A}} T_{\text{A} \rightarrow \text{B}}} \begin{bmatrix} G_{\text{A}} + T_{\text{B} \rightarrow \text{A}} G_{\text{B}} \\ T_{\text{A} \rightarrow \text{B}} G_{\text{A}} + G_{\text{B}} \end{bmatrix}. \quad (\text{B18})$$

Let us now assume that the bodies are perfect spheres of radii  $r_{\text{A}}$  and  $r_{\text{B}}$  and their centers separated by distance  $d$ , as depicted in Fig. 5. We set the intrinsic exitance  $F_{0,b}$  to be constant over the surface for each star separately. We are interested in the

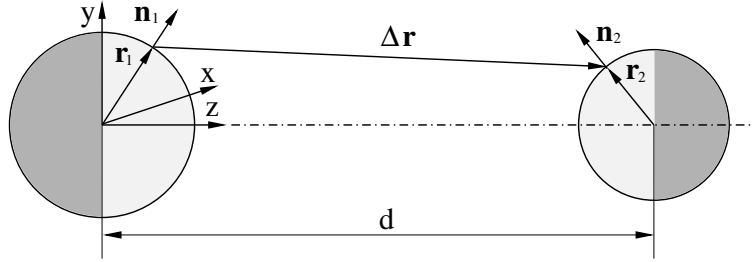


**Figure 5.** Scheme of two spheres used in 1D irradiation model.

limit  $r_b \ll d$  in which we can approximate model constants as

$$L_{l,b \rightarrow b'} \approx \frac{r_b^2}{2d^2}, \quad (\text{B19})$$

$$\eta_b \approx \begin{cases} \frac{1}{2} & : \text{global or latitudinal redistribution} \\ 1 & : \text{local} \end{cases}. \quad (\text{B20})$$

We find numerically that the coefficient  $L_{l,b \rightarrow b'}$  is independent of the type of energy diffusion, labeled by  $l$ . An explicit formula for the coefficient is given in Sec. B.3. In the following we compare the average exiting radiosity  $\langle F_{\text{out},b} \rangle$  and average updated exitance  $\langle F'_{0,b} \rangle$  as function of distance  $d$  between the bodies obtained in one-dimensional model, given by

$$\langle F_{\text{out},b} \rangle = F_{0,b} + \frac{1}{2} \langle F_{\text{in},b} \rangle_{\text{day}}, \quad (\text{B21})$$

$$\langle F'_{0,b} \rangle = F_{0,b} + \frac{1}{2} (1 - \rho_b) \langle F_{\text{in},b} \rangle_{\text{day}}, \quad (\text{B22})$$

and that obtained from numerical calculations by discretizing surface into triangles, as described in Sec. 5. In the considered limit we may take the area of day and night side to be identical, for details see Sec. B.3. The results are depicted in Fig. 6 and show a good qualitative agreement between the two approaches, especially in the limit of larger separations between bodies.

### B.3. Coefficients in 1D model for two-spheres system

Let us consider a binary system composed of two spheres, labeled by A and B, with radii,  $r_{\text{A}}$  and  $r_{\text{B}}$ , and their centers separated by distance  $d$ , as depicted in Fig. 5. The

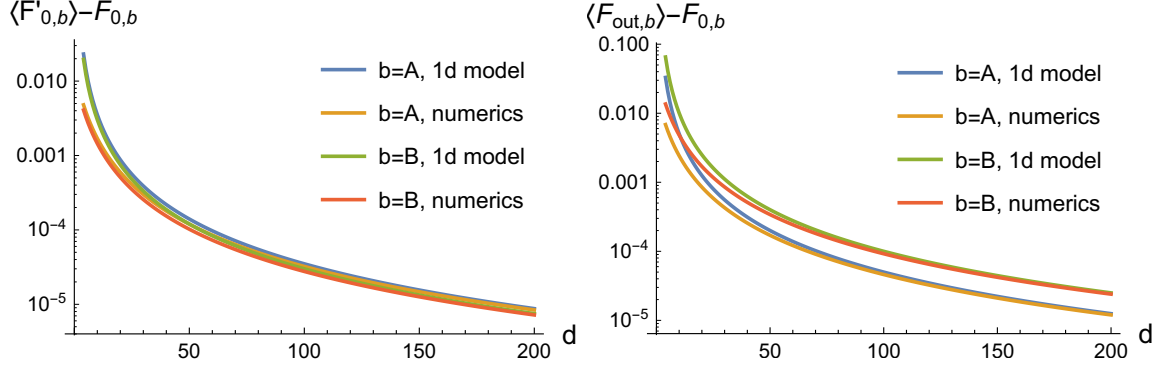


**Figure 6.** Comparing the average updated exitance  $\langle F'_{0,b} \rangle$  (left) and average radiosity  $\langle F_{\text{out},b} \rangle$  (right) obtained from numerical calculations using 10k+ triangles with linear limb-darkening ( $D(\mu) = 1 - x(1 - \mu)$  with  $x = 0.3$ ) and one-dimensional model using global redistribution at parameters  $r_A = 2$ ,  $r_B = 1$ ,  $\eta_A = \eta_B = 1/2$ ,  $F_{0,A} = 1$ ,  $F_{0,B} = 2$ ,  $\rho_A = 0.3$  and  $\rho_B = 0.7$ .

area of the illuminated side of the sphere  $b$  is given by

$$A_{b,\text{day}} = 2\pi r_b^2 \left( 1 - \frac{r'_b - r_b}{d} \right). \quad (\text{B23})$$

We assume that the limb-darkening law is constant across the surface. The coefficients  $L_{l,b \rightarrow b'}$  with  $l = L, \text{LD}$  introduced in Sec. B describing the effect of radiosity operator on the average incoming radiosity can be based on previous subsection identified as the averages of radiosity operator:

$$\left\langle \widehat{\mathcal{L}}_{l,b \rightarrow b'} \right\rangle_{\text{day}} \equiv L_{l,b \rightarrow b'}. \quad (\text{B24})$$

In the considered case this coefficient can be expressed as an integral over all possible pairs points on the two spheres with their line-of-sight unobstructed:

$$L_{l,b \rightarrow b'} = \frac{(r_b r_{b'})^2}{A_{b',\text{day}}} \int d\Omega(\hat{\mathbf{n}}_b) \int d\Omega(\hat{\mathbf{n}}_{b'}) U(\Delta \mathbf{r} \cdot \hat{\mathbf{n}}_b) U(\Delta \mathbf{r} \cdot \hat{\mathbf{n}}_{b'}) \cdot \frac{(\Delta \mathbf{r} \cdot \hat{\mathbf{n}}_b)(\Delta \mathbf{r} \cdot \hat{\mathbf{n}}_{b'})}{\|\Delta \mathbf{r}\|^4} \frac{D_l(\widehat{\Delta \mathbf{r}} \cdot \hat{\mathbf{n}}_b)}{D_{l,0}}, \quad (\text{B25})$$

where integrations is carried out over full solid angles and we should remind ourselves that  $D_l$  is the limb-darkening function and  $D_{l,0}$  its integral over a hemisphere:

$$D_{l,0} = 2\pi \int_0^1 d\mu D_l(\mu) \mu. \quad (\text{B26})$$

Here we use the unit-step function  $U(x) = \{1 : x \geq 0; 0 : \text{otherwise}\}$  and the vector connecting the pairs of points is equal to

$$\Delta \mathbf{r} = r_2 \hat{\mathbf{n}}_2 + d \hat{\mathbf{k}} - r_1 \hat{\mathbf{n}}_1. \quad (\text{B27})$$

We find numerically that the leading order of the average operator in the limit  $d \rightarrow \infty$  behaves as

$$L_{l,b \rightarrow b'} \sim \frac{r_b^2}{2d^2},$$

and this behavior seems to be independent of chosen limb-darkening law labeled by index  $l$ .